

# KINETICS OF GRAIN REFINEMENT IN METALLIC MATERIALS DURING LARGE STRAIN DEFORMATION

A. Belyakov<sup>1</sup>, S. Zherebtsov<sup>2\*</sup>, M. Tikhonova<sup>1</sup>, G. Salishchev<sup>2</sup>

<sup>1</sup>Laboratory of Mechanical Properties of Nanostructured Materials and Superalloys, Belgorod State University, Pobeda 85, Belgorod, 308015, Russia

<sup>2</sup>Laboratory of Bulk Nanostructured Materials, Belgorod State University, Pobeda 85, Belgorod, 308015, Russia

\*e-mail: zherebtsov@bsu.edu.ru

**Abstract.** The development of ultrafine grained microstructures in austenitic stainless steel and pure titanium subjected to large strain deformation was comparatively studied. The change in the volume fractions of newly developed ultrafine grains was used to quantify the progress in grain refinement during plastic deformation. The grain refinement kinetics could be expressed by a modified Johnson-Mehl-Avrami-Kolmogorov equation as a function of true strain. The grain refinement kinetics was suggested being sensitively depended on the deformation conditions and the deformation mechanisms operating during severe plastic working. Under conditions of warm working, an increase in the deformation temperature accelerated dynamic recovery and, therefore, promoted the new grain development. Under conditions of cold working, the grain subdivision in austenitic stainless steel and titanium during cold working was assisted by the deformation twinning. However, the kinetics of grain refinement in austenitic stainless steel was faster as compared to pure titanium owing to strain-induced martensitic transformation.

## 1. Introduction

The thermo-mechanical treatments involving severe plastic deformations have been suggested as very effective methods for processing the ultrafine grained metallic materials [1, 2]. An interest in the ultrafine grained steels and alloys is motivated by a beneficial combination of mechanical properties including high strength with sufficient ductility, which are inherent in such materials [3-6]. However, practical applications of severe plastic deformations require comprehensive knowledge of the mechanisms and regularities of strain-induced evolution of new ultrafine grained microstructures in various metals and alloys.

The development of new grains in metallic materials during plastic deformations is commonly discussed in terms of dynamic recrystallization (DRX) [7]. It has been shown for hot working conditions that the progress in discontinuous DRX obeys normal Avrami kinetics and the recrystallized fraction ( $F_{DRX}$ ) can be related to a strain ( $\epsilon$ ) through a modified Johnson-Mehl-Avrami-Kolmogorov (JMAK) equation [8],

$$F_{DRX} = 1 - \exp(-k(\epsilon - \epsilon_c)^n), \quad (1)$$

where  $k$ ,  $n$  and  $\epsilon_c$  are constants, which depend on material and processing conditions. The dynamic grain size evolved by discontinuous DRX during hot working can be expressed by a power law function of flow stress with stress exponent of about -1.5 [9]. This dependence suggests that ultrafine grained structures with submicrometer or even nanometer grain size can be developed in metallic materials during plastic deformation at relatively low

temperatures. In contrast to hot working conditions, however, the process of dynamic recrystallization under cold to warm deformation conditions has not been studied in sufficient detail. Generally, the kinetics of dynamic recrystallization development slows down as the deformation temperature decreases. The discontinuous DRX can be completely suppressed under conditions of cold to warm deformation. In such cases, the development of new ultrafine grains during deformation has been discussed as a result of so-called continuous DRX [7]. The change in recrystallization mechanism results in variation of power law relationship between the flow stress and dynamic grain size [10]. On the other hand, the kinetics of DRX developing under cold to warm deformation conditions has not been studied quantitatively. Therefore, the aim of the present paper is to study the effect of deformation conditions and materials on the grain refinement kinetics and clarify the applicability of modified JMAK equation to quantitative evaluation of continuous recrystallization development.

## 2. Experimental Procedure

An S304H austenitic stainless steel (Fe-0.10 C-18.2 Cr-7.85 Ni-2.24 Cu-0.50 Nb-0.008 B-0.12 N-0.95 Mn-0.10 Si, all in wt.%) with an initial grain size of about 7  $\mu\text{m}$ , a 304-type austenitic steel (Fe-0.05% C-18.2% Cr-8.8% Ni-1.65% Mn-0.43% Si-0.05% P-0.04% S, all in wt%) with an initial grain size of 21  $\mu\text{m}$  and a commercial-purity titanium (impurities in wt.% less than: 0.18 Fe, 0.1 Si, 0.07 C, 0.04 N, 0.01 H, 0.12 O) with a grain size of 15  $\mu\text{m}$ , were used. The large strain deformations were carried out by multiple multidirectional forging or plate rolling. The multidirectional forging (warm deformation) was carried out by means of isothermal multi-pass compression tests at temperatures of 773-973 K using prismatic samples with initial dimension of  $10 \times 12.2 \times 15 \text{ mm}^3$  [11]. Plate rolling (cold deformation) was carried out at room temperature. The structural investigations were carried out on the sample sections parallel to the compression axis of the final forging pass of the multiply forged samples or on the transverse planes (i.e., the sections normal to the transverse direction) of the cold rolled steel samples and on the normal planes (i.e., the sections normal to the normal direction) of the cold rolled titanium samples using a JEOL JEM-2100 transmission electron microscope (TEM) and an FEI Quanta 600F scanning electron microscope equipped with an electron back scatter diffraction (EBSD) analyzer. The EBSD patterns were subjected to clean-up procedures, setting a minimal confidence index of 0.1. The grain refinement kinetics was studied by means of unique grain color mappings where individual grains bounded by high-angle boundaries with misorientations of  $\theta \geq 15^\circ$  are indicated by different colors. The volume fraction of ultrafine grains was deemed to be the DRX fraction. The fraction of strain-induced martensite in the cold rolled austenitic stainless steel was averaged through X-ray analysis, magnetic induction method and EBSD technique.

## 3. Results and Discussion

### 3.1. Temperature effect on grain refinement kinetics during warm deformation.

The structural changes in an S304H stainless steel during warm multidirectional forging have been described in general elsewhere [11]. The present paper focuses on the detailed quantitative evaluation of the development of ultrafine grains. Typical deformation microstructures evolved in an S304H stainless steel during multiple multidirectional forging at 773 K are shown in Fig. 1. The first forging pass ( $\epsilon = 0.4$  in Fig. 1) flattens the original grains; any new fine grains can scarcely be observed.

Further subsequent forging to total strain of 1.2 results in the development of a number of strain-induced grain boundaries, which is essential feature of continuous DRX [7]. The new ultrafine grains frequently develop along original grain boundaries and their triple junctions, where large strain gradients and corresponding high density of strain-induced boundaries

evolve. The number of new fine grains and their volume fraction increase as total strain increases. Thus, the ultrafine grained structure occupies almost all volume after ten forging passes ( $\epsilon = 4.0$  in Fig. 1).

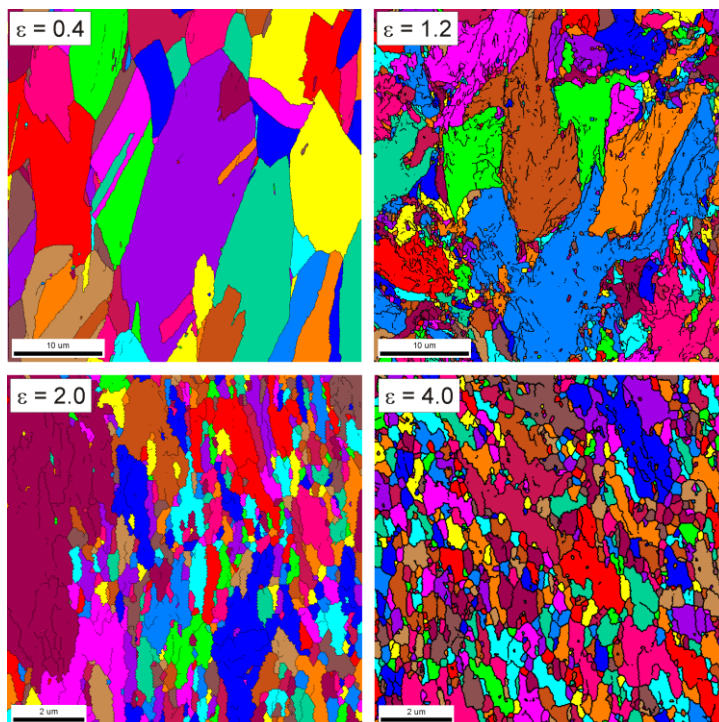


**Fig. 1.** Unique grain color mappings of deformation microstructures developed in an S304H stainless steel during multiple multidirectional forging at 773 K.

The formation of strain-induced ultrafine grains during the multiple forging can be clearly tracked by the change in the grain size distributions (Fig. 2).

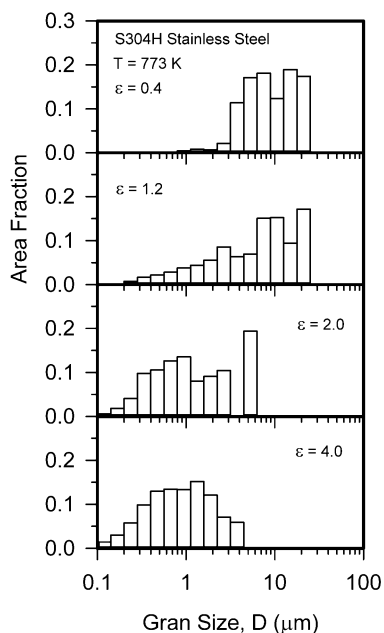


**Fig. 2.** Grain size distributions in an S304H stainless steel subjected to multiple multidirectional forging at 773 K.

A huge peak corresponding to rather coarse original grains is clearly seen in the grain size distribution evolved at a relatively small total strain of 0.4. Upon further multiple forging,

the height of this peak decreases and the peak spreads out towards small grain sizes as a result of progressive development of new ultrafine grains. It should be noted that a kind of bimodal grain size distribution with two peaks against small and large grain sizes evolve at intermediate strains. It is evident that the gradual development of new ultrafine grains results in the growing peak at small grain sizes, whereas the peak at large grain sizes corresponds to coarse remnants of original grains. The former fraction increases while that of the latter decreases with straining. Finally, a peak corresponding to the new ultrafine grains stands up in the grain size distribution evolved at sufficiently large total strains.

An increase in the temperature of multiple multidirectional forging does not lead to qualitative changes in the sequence of structural changes in an S304H stainless steel. The flattened original grains with their frequently serrated boundaries evolve at an early deformation ( $\epsilon = 0.4$  in Fig. 3). Then, the curly mixed microstructure consisting of irregular shaped remnants of original grains and the strain-induced ultrafine grains evolves during subsequent forging (s.  $\epsilon = 1.2$  in Fig. 3). The multiple forging at higher temperature is characterized by a faster increase in the fraction of ultrafine grains. The fraction of ultrafine grains in the deformation microstructure of steel sample subjected to multiple forging at 973 K to a total strain of 2 comprises about 0.9, whereas that of about 0.6 was observed at 773 K after the same strain level. Therefore, an increase in deformation temperature promotes the development of continuous DRX during large strain warm deformation.

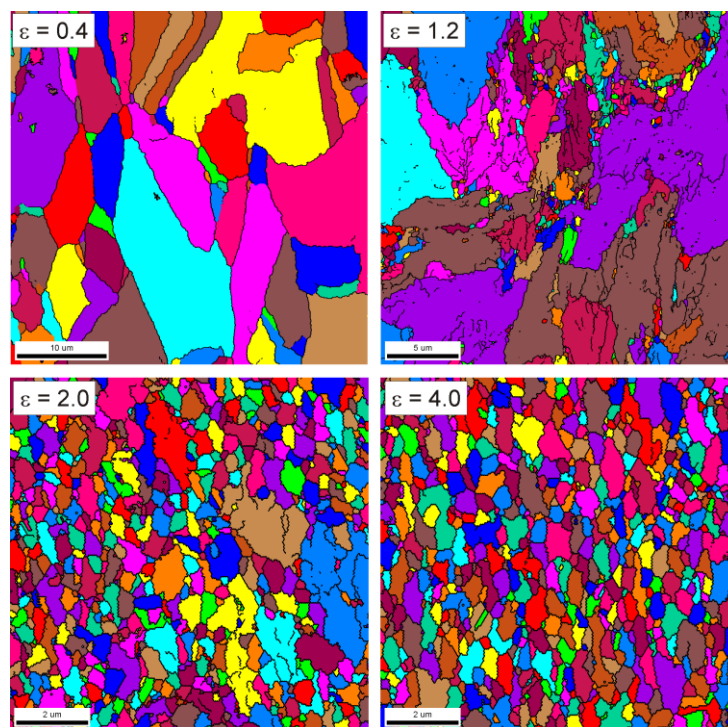


**Fig. 3.** Unique grain color mappings of deformation microstructures developed in an S304H stainless steel during multiple multidirectional forging at 973 K.

The corresponding grain size distributions in an S304H stainless steel subjected to warm multiple forging at 973 K are shown in Fig. 4. Again, it is clearly seen that the multiple forging at 973 K results in gradual replacement of a coarse grain peak with an ultrafine grain one through bimodal grain size distributions at intermediate strains. Such changes in the grain size distribution have been frequently observed during discontinuous DRX leading to grain refinement during hot working [12]. Therefore, the changes in the grain size distributions upon the progress in dynamic recrystallization under conditions of warm or hot deformation are almost the same in spite of different mechanisms of the new grain development.

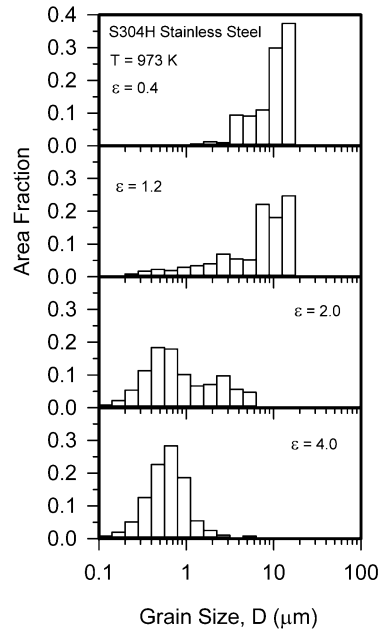


**Fig. 4.** Grain size distributions in an S304H stainless steel subjected to multiple multidirectional forging at 973 K.

Quantitatively, the kinetics of discontinuous DRX during hot working can be expressed by Eq. (1). In this case, the plot of  $\ln(1/(1-F_{\text{DRX}}))$  vs  $\epsilon$  in logarithmic scale should represent a straight line. Figure 5 shows the  $\log(\ln(1/(1-F_{\text{DRX}})))$  vs  $\log(\epsilon)$  relationship for the present study on the development of ultrafine grains due to continuous DRX in an S304H stainless steel subjected to large strain warm deformation. It is clearly from Fig. 5 that the progress in the grain refinement during warm multiple forging of an S304H stainless steel can be expressed by a modified JMAK equation (Eq. (1)), where critical strain for DRX initiation is near zero. The strain effect on the recrystallized fraction in an S304H stainless steel subjected to multiple forging at different temperatures is shown in Fig. 6. The solid lines represent the recrystallized fractions calculated by modified JMAK equations, setting the obtained in Fig. 5 parameters. It is clearly seen that an increase in deformation temperature from 773 K to 873 K (0.4-0.5  $T_m$ , where  $T_m$  is the melting point) does not lead to any remarkable changes in the grain refinement kinetics, whereas further increase of temperature to 973 K (0.56  $T_m$ ) results in significant acceleration of continuous DRX. Similar DRX behavior has been reported for warm rolling [13].

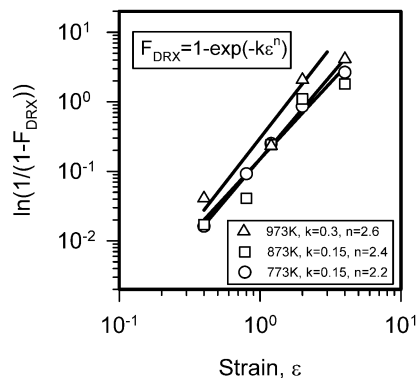


**Fig. 5.** Relationship between  $\ln(1/(1-F_{\text{DRX}}))$  and strain for an S304H stainless steel subjected to multiple multidirectional forging at 773-973 K.

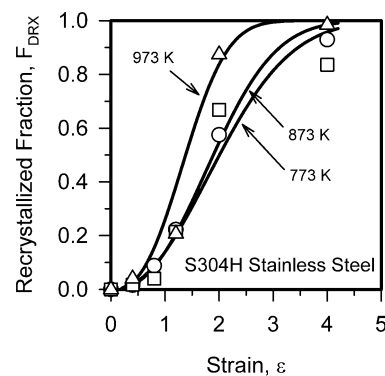


**Fig. 6.** Increase in the recrystallized fraction in an S304H stainless steel during warm multiple deformation.

**3.2. Grain refinement kinetics during large strain cold deformation.** The grain refinement kinetics during large strain cold working were studied by using the samples of stainless steel and titanium, which were subjected to plate rolling at ambient temperature. Figure 7 shows typical deformation microstructures developed in a 304-type stainless steel during cold rolling. The structural changes are characterized by the development of deformation twinning and microshear-banding at relatively small strains followed by the strain-induced martensitic transformation at moderate strains as detailed elsewhere [14].

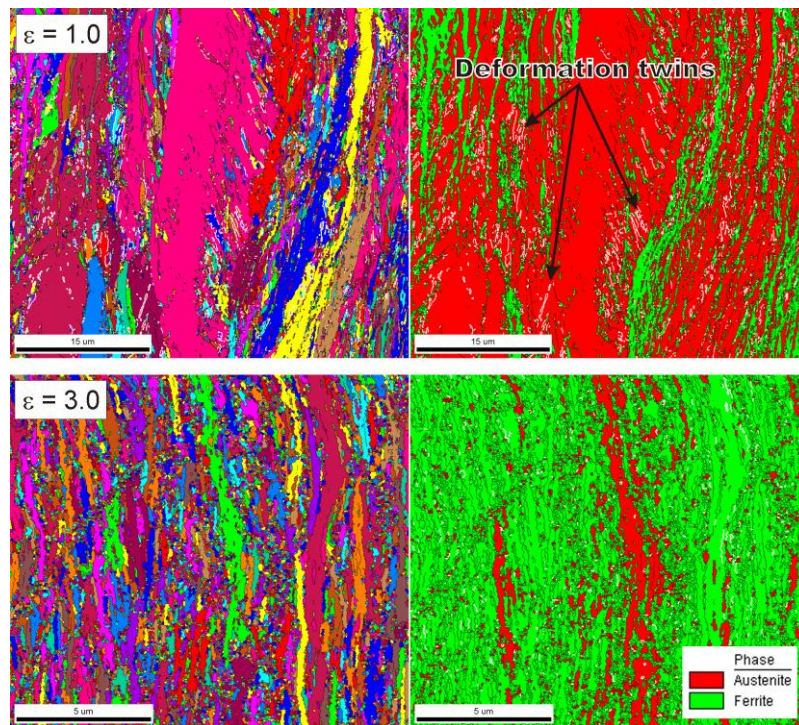


**Fig. 7.** Unique grain color mappings of deformation microstructures (left micrographs) and phase distributions (right micrographs) developed in a 304-type stainless steel during plate rolling at room temperature. Deformation twins are indicated by white lines.

The latter readily develops at moderate strains leading the martensite fraction to approach about 0.8 at a large strain of 3 (Fig. 8).

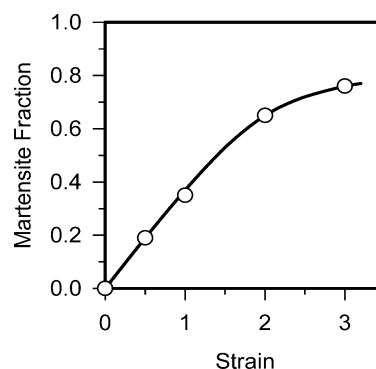


**Fig. 8.** The effect of cold rolling strain on the fraction of strain-induced martensite in a 304-type stainless steel.

Both the deformation twinning and the martensitic transformation result in rapid grain refinement. The fraction of ultrafine grains comprises about 0.9 at a total strain of 3 ( $\epsilon = 3.0$  in Fig. 7). Typical deformation microstructures developed in titanium during cold rolling are shown in Fig. 9. The structural changes in commercial-purity titanium during cold rolling

have been described in details using TEM and EBSD elsewhere [15-17]. The titanium samples are also susceptible to intensive deformation twinning during cold working. It is clearly seen in Fig. 9 that many ultrafine grains with a size of about 100 nm readily develop in titanium during cold rolling, although the grain refinement kinetics in titanium is noticeably slower than that in austenitic stainless steel. The fraction of ultrafine grains in titanium comprises about 0.4 at a total strain of 2.66.

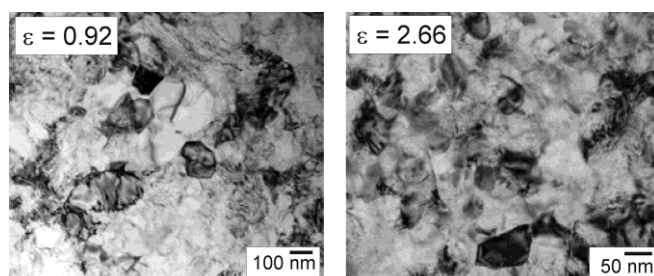


**Fig. 9.** TEM images of deformation structures developed in a pure titanium during plate rolling at room temperature.

The relationships between  $\ln(1/(1-F_{DRX}))$  and rolling strain for pure titanium and stainless steel subjected to cold rolling at room temperature are shown in Fig. 10a. The data for ultrafine grain fractions obtained by Tsuji's group on a pure titanium during cold accumulated roll bonding (ARB) [18] are also included in this figure for reference. The above relationships can be represented by linear functions in log-log scale. This suggests that the grain refinement kinetics in austenitic steel and titanium during cold rolling (as well as ARB processing) can be accurately evaluated by a modified JMAK equation (Eq. (1)). The results of such calculations are displayed in Fig. 10b by solid lines. The DRX fractions (the fraction of ultrafine grains) calculated by Eq. (1) match well the experimental results. It can be concluded, therefore, that the grain refinement kinetics can be adequately described in terms of the Johnson-Mehl-Avrami-Kolmogorov model even for cold working. The difference in the grain refinement kinetics in austenitic stainless steel and titanium during cold rolling can result from strain-induced phase transformation, which provides an extra contribution to grain refinement in austenitic stainless steel.

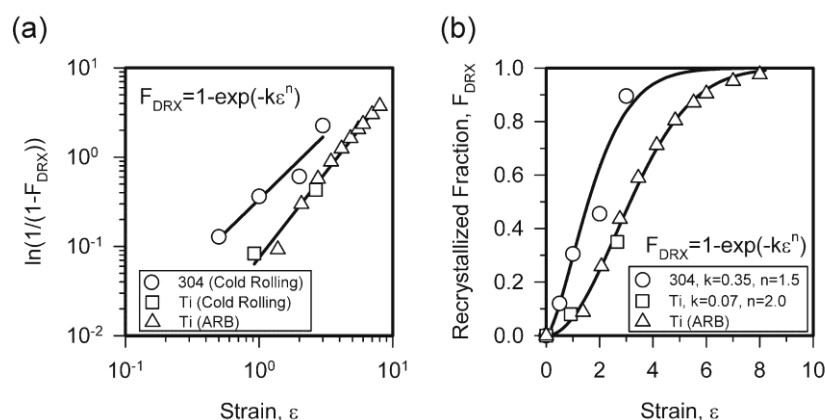


**Fig. 10.** The strain effect on the dynamic recrystallization in a 304-type stainless steel and pure titanium during cold rolling at room temperature,  $\ln(1/(1-F_{DRX}))$  vs  $\epsilon$  (a) and  $F_{DRX}$  vs  $\epsilon$  (b). The data for ARB were taken from [18].

#### 4. Summary

The development of new ultrafine grains in austenitic stainless steel and titanium during large strain cold to warm deformation results from strain-induced continuous reactions and can be

considered as a kind of continuous dynamic recrystallization. The kinetics of grain refinement during large strain cold to warm working can be expressed by a modified Johnson-Mehl-Avrami-Kolmogorov equation much similar to conventional dynamic recrystallization taking place in various metallic materials during hot working. An increase in deformation temperature in the low temperature domain of warm working (below about 0.5  $T_m$ ) does not change the grain refinement kinetics remarkable, whereas an increase in the temperature well above 0.5  $T_m$  accelerates the kinetics of continuous dynamic recrystallization. The grain subdivision in austenitic stainless steel and titanium during cold working is assisted by the deformation twinning (in both austenite and titanium) and strain-induced martensitic transformation (in austenite), which increase the rate of grain refinement.

### **Acknowledgements**

*The studies on austenitic stainless steels were carried out by A. Belyakov and M. Tikhonova under financial support received from the Ministry of Education and Science, Russia (grant No. 14.575.21.0070, ID No. RFMEFI57514X0070). The studies on titanium were carried out by S. Zharebtsov and G. Salishchev under financial support received from the Ministry of Education and Science, Russia (grant No. 11.1816.2014/K). The authors are grateful to the personnel of the Joint Research Centre, Belgorod State University, for their assistance with instrumental analysis.*

### **References**

- [1] R.Z. Valiev, R.K. Islamgaliev, I.V. Alexandrov // *Progress in Materials Science* **45** (2000) 103.
- [2] Y. Estrin, A. Vinogradov // *Acta Materialia* **61** (2013) 782.
- [3] R.Z. Valiev, T.G. Langdon // *Advanced Engineering Materials* **12** (2010) 677.
- [4] S.V. Dobatkin, V.F. Terent'ev, W. Skrotzki, O.V. Rybalchenko, M.N. Pankova, D.V. Prosvirnin, E.V. Zolotarev // *Russian Metallurgy (Metally)* **2012** (2012) 954.
- [5] G.A. Salichshev, R.M. Galeev, S.P. Malysheva, S.V. Zharebtsov, S.Yu. Mironov, O.A. Valiakhmetov and E.I. Ivanisenko // *Metal Science and Heat Treatment* **48** (2006) 63.
- [6] S. Zharebtsov, E. Kudryavtsev, S. Kostjuchenko, S. Malysheva, G. Salishchev // *Materials Science and Engineering A* **536** (2012) 190.
- [7] T. Sakai, A. Belyakov, R. Kaibyshev, H. Miura, J.J. Jonas // *Progress in Materials Science* **60** (2014) 130.
- [8] W. Roberts, In: *Strength of Metals and Alloys (ICSMA-7)*, ed. by H.J. McQueen et al. (Pergamon Press, Oxford, UK, 1986), p. 1859.
- [9] B. Derby // *Acta Metallurgica et Materialia* **39** (1991) 955.
- [10] A. Belyakov, S. Zharebtsov, G. Salishchev // *Materials Science and Engineering A* **628** (2015) 104.
- [11] M. Tikhonova, A. Belyakov, R. Kaibyshev // *Materials Science and Engineering A* **564** (2013) 413.
- [12] F.J. Humphreys, M. Hatherly, *Recrystallization and Related Annealing Phenomena* (Elsevier, Oxford, 2004).
- [13] Z. Yanushkevich, A. Belyakov, R. Kaibyshev // *Acta Materialia* **82** (2015) 244.
- [14] M. Odnobokova, A. Belyakov, R. Kaibyshev // *Metals* **5** (2015) 656.
- [15] S.V. Zharebtsov, G.S. Dyakonov, A.A. Salem, V.I. Sokolenko, G.A. Salishchev, S.L. Semiatin // *Acta Materialia* **61** (2013) 1167.
- [16] S.V. Zharebtsov, G.S. Dyakonov, A.A. Salem, S.P. Malysheva, G.A. Salishchev, S.L. Semiatin // *Materials Science and Engineering A* **528** (2011) 3474.
- [17] G.S. Dyakonov, S. Mironov, S.V. Zharebtsov, S.P. Malysheva, G.A. Salishchev, A.A. Salem, S.L. Semiatin // *Materials Science and Engineering A* **607** (2014) 145.
- [18] D. Terada, S. Inoue, N. Tsuji // *Journal of Materials Science* **42** (2007) 1673.